

Studying and Analysis of the Characteristic of the High-Order and MRTD and RK-MRTD Schemes

Min Zhu, Qunsheng Cao, and Siping Gao

College of Electronic and Information Engineering
Nanjing University of Aeronautics and Astronautics, Nanjing 210016, China
minzhu215@gmail.com and qunsheng@nuaa.edu.cn

Abstract — In this paper, the stability, dispersion, and convergence of the high-order FDTD (HO-FDTD), the multi-resolution time-domain (MRTD), and the Runge-Kutta multi-resolution time-domain (RK-MRTD) schemes are derived, analyzed, and compared. The computational cost and memory requirements of the three methods are also investigated. It is found that the RK-MRTD method is of considerable potential due to its dispersion properties and computational abilities.

Index Terms — Convergence, dispersion, HO-FDTD, MRTD, RK-MRTD, and stability.

I. INTRODUCTION

The classical Yee FDTD [1] method has become the most important numerical technique in the computational electromagnetics time domain over the past few decades, and has been applied widely to simulate electromagnetic wave propagation, scattering, radiation, and various microwave geometries, owing to its simple implementation and versatility. However, the technique suffers from serious limitations due to the substantial computer resources required when it involves modeling a complex problem, which has large stencil size at least 10 cells or more per wavelength. It is well known that the FDTD method has a second order accuracy in spatial-temporal and brought significant computational errors. In order to improve the limitations of the FDTD method, a mass of methods are proposed, including the HO-FDTD [2-4], the MRTD [5], the RK-MRTD method [6] have been raised. The HO-FDTD approach, firstly presented by Fang [2], using the Taylor series instead of the spatial and

temporal derivatives to reducing the dispersion error. It is noted that the HO-FDTD method adopted a second-order approximation in time, fourth-order accurate in space-domain called HO-FDTD (2, 4) scheme, and the HO-FDTD (2, 6) with sixth-order in space and second-order in time was developed to deal with the electric large size problem [3]. Zhang and Chen [7] put forward to the general updated equations and dispersion relations for the arbitrary HO-FDTD (2N, 2M). The fourth-order accurate FDFD scheme is proposed and applied in the waveguide structures. The results demonstrate that the proposed method can save more time and memory than MRFD and the traditional FDFD methods [8]. The MRTD method, introduced by Krumpholz and Katehi, are based mainly on the filed expansions of different basis scaling and wavelet function, such as the Battle-Lemarie [9-10] basis, the Daubechies basis [11], Cohen - Daubechies - Feauveau (CDF) bi-orthogonal functions [12, 13] basis, and Coifman function basis [14, 15]. In [16], Cao and Tamma discussed the MRTD method based on different scaling function expansions, and computed the reflected and transmission coefficients for stratified slab media, and the results show that the cubic spline Battle-Lemarie, Daubechies D4 and Coiflet bases are in excellent agreement with the analytic solutions. Cao and Tamma also applied the MRTD methods based on different basis functions to study the scattering of planar stratified medium and rectangular dielectric cylinder [17]. In [18] the MRTD method has been discussed in detail, especially a non-uniform Cartesian grid and a uniaxial perfectly matched layer implementation for arbitrary levels of wavelet resolution. A procedure to implement the PML absorbing

boundary conditions into the MRTD method based on the discrete wavelet transform has been developed in [19]. The strong stability Runge-Kutta (SSP-RK) method was first introduced and extended in [20] and [21]. Compactly supported n^{th} -order wavelets and m^{th} -order, m^{th} -stage Runge-Kutta are applied in spatial discretization and time integration, respectively. Numerical experiments have shown that much better numerical dispersion properties are obtained by employing the RK-MRTD scheme.

In summary, the HO-FDTD, the MRTD, and the RK-MRTD methods are the high order accuracy time domain methods and have extremely low numerical dispersion errors. In section II, the update equations of the HO-FDTD, the MRTD, and the RK-MRTD schemes are discussed. The numerical properties of the HO-FDTD, the MRTD, and the RK-MRTD methods are derived including stability conditions, dispersion relation, and convergence in section III. The computational cost and memory requirements of the three schemes are investigated in section IV. In section V, a numerical example will be simulated for different methods. Conclusions are summarized in section VI.

II. THEORY AND ALGORITHM

A. HO-FDTD method

For simplicity ($\sigma = 0$) and without loss of generality, in three-dimensional (3D), one update equation of the arbitrary HO-FDTD ($2N, 2M$) [7] can be written as,

$$\begin{aligned} E_{x,i+1/2,j,k}^{n+N} = & E_{x,i+1/2,j,k}^{n+1-N} - \frac{1}{a(N)} \sum_{v=1}^{N-1} a(v) (E_{x,i+1/2,j,k}^{n+v} - E_{x,i+1/2,j,k}^{n+1-v}) + \\ & \frac{\Delta t}{a(N)\varepsilon\Delta y} \sum_{v=1}^M a(v) (H_{z,i+1/2,j-1/2+v,k}^{n+1/2} - H_{z,i+1/2,j+1/2-v,k}^{n+1/2}) - \\ & \frac{1}{a(N)} \frac{\Delta t}{\varepsilon\Delta z} \sum_{v=1}^M a(v) (H_{y,i+1/2,j,k-1/2+v}^{n+1/2} - H_{y,i+1/2,j,k+1/2-v}^{n+1/2}) \end{aligned} \quad (1)$$

where Δt , Δy , and Δz are the time step size and the spatial step size in the y- and z-directions, $2N$ means the $(2N)^{\text{th}}$ -order central difference approximation in time domain, $2M$ is the $(2M)^{\text{th}}$ -order in space time, ε is the permittivity, and the coefficients $a(v)$ [7] are listed in Table 1. We note that the HO-FDTD ($2, 2M$) equations are similar

to the MRTD method. Here in this paper, we mainly discuss the HO-FDTD ($2, 2M$) scheme.

B. MRTD method

Similarly, considering the same electromagnetic condition as the HO-FDTD method, one update equation of the MRTD scheme based on Daubechies scaling functions [6] can be written as follows,

$$\begin{aligned} E_{i+1/2,j,k}^{\phi x,n+1} = & E_{i+1/2,j,k}^{\phi x,n} + \frac{1}{\varepsilon} \sum_v a(v) \\ & \times \left(H_{i+1/2,j+v+1/2,k}^{\phi z,n+1/2} \frac{\Delta t}{\Delta y} - H_{i+1/2,j,k+v+1/2}^{\phi y,n+1/2} \frac{\Delta t}{\Delta z} \right) \end{aligned} \quad (2)$$

where Δx , Δy , Δz , and Δt represent the space and time discretization intervals in x-, y-, z- and t-directions, respectively, and ϕ refers to the Daubechies or Coifman scaling functions, ε is the permittivity, and the coefficients $a(v)$ are listed in Table 2 for Daubechies (D2), (D3), and (D4) schemes [6] and Coifman scheme [14], and the coefficients $a(v)$ have the symmetric relations, namely, $a(-v) = -a(v-1)$.

C. RK-MRTD method

For the same conditions above, one update equation of the RK-MRTD scheme [6], which is based on the same convergence rate for the time and space, can be written as,

$$\begin{aligned} \frac{\partial_{\phi x} E_{i+1/2,j,k}(t)}{\partial t} = & \frac{1}{\varepsilon} \sum_v a(v) \times \\ & \left(\phi_z H_{i+1/2,j+v+1/2,k}(t) \frac{1}{\Delta y} - \phi_y H_{i+1/2,j,k+v+1/2}(t) \frac{1}{\Delta z} \right) \end{aligned} \quad (3)$$

where the coefficients $a(v)$ is the same as the MRTD method listed in Table 2.

The general form for equation (3) as in [6], can be written as

$$\frac{\partial F}{\partial t} = uF + S(t), \quad (4)$$

where $F = \{E, H\}^T$, E and H are expressed as $E = \{E_x, E_y, E_z\}^T$, $H = \{H_x, H_y, H_z\}^T$, where T is the transpose of the vector, u is a operator and defined

as $u = \begin{bmatrix} 0 & u_H \\ u_E & 0 \end{bmatrix}$, $S(t)$ is a source, the form of the

m^{th} -order m' stage strong stability preserving Runge-Kutta (SSP-RK) [6] schemes are shown as,

$$\begin{aligned}
 F^{(0)} &= F_n \\
 F^{(i)} &= F^{(i-1)} + \Delta t u F^{(i-1)} + \Delta t S^{(i)}, \quad i=1,2,\dots,m \quad (5) \\
 F_{n+1} &= \sum_{l=0}^m \alpha_{m,l} F^{(l)}
 \end{aligned}$$

where $S^{(i)} = (I + \Delta t \frac{\partial}{\partial t})^{i-1} S(t_n)$, $i=1,2,\dots,m$, I is identity matrix, the coefficients $\alpha_{m,l}$ [6] are,

$$\begin{aligned}
 \alpha_{m,m} &= \frac{1}{m!}, \quad l = m \\
 \alpha_{m,l} &= \frac{1}{l} \alpha_{m-1,l-1}, \quad l = 1,2,\dots,m-1, m \geq 2, \quad (6) \\
 \alpha_{m,0} &= 1 - \sum_{l=1}^m \alpha_{m,l}, \quad l = 0.
 \end{aligned}$$

Now, we use the Fourier method [22] to analyze the stability of the RK-MRTD, following the [23], we solve the update equations of RK-MRTD and obtain,

$$\frac{\partial}{\partial t} \begin{bmatrix} E(t) \\ H(t) \end{bmatrix} = \begin{bmatrix} \mathbf{0} & u_H \\ u_E & \mathbf{0} \end{bmatrix} \begin{bmatrix} E(t) \\ H(t) \end{bmatrix} \quad (7)$$

where

$$E(t) = \begin{Bmatrix} E_x(t) \\ E_y(t) \\ E_z(t) \end{Bmatrix}, \quad H(t) = \begin{Bmatrix} H_x(t) \\ H_y(t) \\ H_z(t) \end{Bmatrix},$$

Table 1: Coefficients $a(v)$ for the HO-FDTD ($2N, 2M$) method.

	(2, 6)	(2, 10)	(2, 14)	(2, 16)
$a(1)$	1.171875	1.211242676	1.228606224	1.23409107
$a(2)$	-0.0651041667	-0.0897216797	-0.102383852	-0.106649846
$a(3)$	0.0046875000	0.0138427734	0.0204767704	0.0230363667
$a(4)$		-0.00176565988	-0.00417893273	-0.0053423856
$a(5)$		0.000118679470	0.000689453549	0.00107727117
$a(6)$			-0.0000769225034	-0.000166418878
$a(7)$			0.00000423651475	0.0000170217111
$a(8)$				-0.000000852346421

Table 2: Coefficients $a(v)$ for the MRTD method.

	D2	D3	D4	Coifman
$a(1)$	1.2291666667	1.2918129281	1.3110340773	1.31103179882954
$a(2)$	-0.0937500000	-0.1371343465	-0.1560100710	-0.15600971692384
$a(3)$	0.0104166667	0.0287617723	0.0419957460	0.04199608161407
$a(4)$		-0.0034701413	-0.0086543236	-0.00865439622799
$a(5)$		0.0000080265	0.0008308695	8.30874303205e-04
$a(6)$			0.0000108999	1.09002750582e-05
$a(7)$			-0.0000000041	-4.10840975298e-09
$a(8)$				-7.977050410221e-13

$$u_E = \begin{bmatrix} 0 & u_{E1} & u_{E2} \\ u_{E3} & 0 & u_{E4} \\ u_{E5} & u_{E6} & 0 \end{bmatrix}, \quad u_H = \begin{bmatrix} 0 & u_{H1} & u_{H2} \\ u_{H3} & 0 & u_{H4} \\ u_{H5} & u_{H6} & 0 \end{bmatrix}, \quad u_{E1} = - \frac{2i \sum_{v=0}^{Nv-1} a(v) \sin(k_z(1/2+v)\Delta z)}{\epsilon \Delta z},$$

the component 0 is a 3 by 3 zero matrix, and $u_{E1}, u_{E2}, u_{E3}, u_{E4}, u_{E5}, u_{E6}, u_{H1}, u_{H2}, u_{H3}, u_{H4}, u_{H5}, u_{H6}$ are

$$\begin{aligned}
u_{E2} &= \frac{2i \sum_{v=0}^{Nv-1} a(v) \sin(k_y(1/2+v)\Delta y)}{\varepsilon \Delta y}, \\
u_{E3} &= \frac{2i \sum_{v=0}^{Nv-1} a(v) \sin(k_z(1/2+v)\Delta z)}{\varepsilon \Delta z}, \\
u_{E4} &= -\frac{2i \sum_{v=0}^{Nv-1} a(v) \sin(k_x(1/2+v)\Delta x)}{\varepsilon \Delta x}, \\
u_{E5} &= -\frac{2i \sum_{v=0}^{Nv-1} a(v) \sin(k_y(1/2+v)\Delta y)}{\varepsilon \Delta y}, \\
u_{E6} &= \frac{2i \sum_{v=0}^{Nv-1} a(v) \sin(k_x(1/2+v)\Delta x)}{\varepsilon \Delta x}, \\
u_{H1} &= \frac{2i \sum_{v=0}^{Nv-1} a(v) \sin(k_z(1/2+v)\Delta z)}{\mu \Delta z}, \\
u_{H2} &= -\frac{2i \sum_{v=0}^{Nv-1} a(v) \sin(k_y(1/2+v)\Delta y)}{\mu \Delta y}, \\
u_{H3} &= -\frac{2i \sum_{v=0}^{Nv-1} a(v) \sin(k_z(1/2+v)\Delta z)}{\mu \Delta z}, \\
u_{H4} &= \frac{2i \sum_{v=0}^{Nv-1} a(v) \sin(k_x(1/2+v)\Delta x)}{\mu \Delta x}, \\
u_{H5} &= \frac{2i \sum_{v=0}^{Nv-1} a(v) \sin(k_y(1/2+v)\Delta y)}{\mu \Delta y}, \\
u_{H6} &= -\frac{2i \sum_{v=0}^{Nv-1} a(v) \sin(k_x(1/2+v)\Delta x)}{\mu \Delta x}. \quad (8)
\end{aligned}$$

We use the characteristic equation to solve u for equation (7) and be obtained as follows,

$$\begin{aligned}
|\lambda I - u| &= \lambda^6 + 8c^2 \lambda^4 \left[(\xi_x)^2 + (\xi_y)^2 + (\xi_z)^2 \right] \\
&+ 16c^4 \lambda^2 \left[2(\xi_x \xi_y)^2 + 2(\xi_x \xi_z)^2 + 2(\xi_y \xi_z)^2 \right. \\
&\left. + (\xi_x)^4 + (\xi_y)^4 + (\xi_z)^4 \right] = 0 \quad (9)
\end{aligned}$$

$$\xi_\tau = \frac{\sum_{v=0}^{Nv-1} a(v) \sin(k_\tau(1/2+v)\Delta \tau)}{\Delta \tau}, \quad (10)$$

where $i = \sqrt{-1}$, $\tau = x, y, z$, the positive part of the Eigen value for u can be derived as,

$$\lambda = i2c\sqrt{(\xi_x)^2 + (\xi_y)^2 + (\xi_z)^2} = i\lambda' \quad (11)$$

where c is the speed of light in vacuum in this paper, λ' is the imaginary part of λ .

III. NUMERICAL PROPERTIES

A. Stability

Based on the stability condition of the Yee's FDTD with the uniform discretization size $\Delta x = \Delta y = \Delta z = \Delta l$, the HO-FDTD (2N, 2M) stability condition can be derived as,

$$\Delta t \leq \frac{\Delta l \left(\sum_{v=1}^N |a(v)| \right)}{c \left(\sum_{v=1}^M |a(v)| \right) \sqrt{d}}. \quad (12)$$

We only discuss the HO-FDTD (2, 2M) case, so the stability condition relation above can be modified as,

$$\Delta t \leq \frac{\Delta l}{c \left(\sum_{v=1}^N |a(v)| \right) \sqrt{d}}. \quad (13)$$

The stability condition for MRTD scheme is derived, as in [11],

$$\Delta t \leq \frac{\Delta l}{c \left(\sum_v |a(v)| \right) \sqrt{d}} \quad (14)$$

where $a(v)$ are listed in Table 2, and d is the number of dimensions (1, 2, or 3).

The RK-MRTD method is based on the SSP-RK algorithm and the MRTD scheme, so the stability condition of the scheme should be considered as the combination of the two algorithms. In reference [20], equation (5) can take the general forms as,

$$F(t_{n+1}) = \sum_{l=0}^{m'} \frac{1}{l!} (\Delta t L) F(t_n) = GF(t_n) \quad (15)$$

where m' is the order of the SSP-RK, L is the spatial amplification matrix of the Eigen value λ , and G is the general growth factor, so the absolute value of G is lower or equal to 1, from equation (15) we can define the growth factor σ [23] as,

$$\sigma = \sum_{l=0}^{m'} \frac{1}{l!} (\lambda \Delta t)^l. \quad (16)$$

If $m' = 4$, then the stability condition of the RK₄-MRTD-D₄ method, which RK _{m'} -MRTD-D _{m'} refers to the m' th-order m' stage SSP-RK method based on Daubechies m' scaling function [24], is obtained as,

$$\left| \sum_{l=0}^4 \frac{1}{l!} (\lambda \Delta t)^l \right| = \left| \sum_{l=0}^4 \frac{1}{l!} (i \lambda' \Delta t)^l \right| \leq 1$$

$$\left| 1 + i \lambda' \Delta t - \frac{1}{2} (\lambda' \Delta t)^2 - \frac{1}{6} (\lambda' \Delta t)^3 + \frac{1}{24} (\lambda' \Delta t)^4 \right| \leq 1$$

$$\lambda' \Delta t \leq 2\sqrt{2}, \quad (17)$$

substituting equations (11) into (17), then the RK₄-MRTD-D₄ stability condition can be derived as,

$$\Delta t \leq \frac{\Delta 2\sqrt{2}}{c(\sum_v |a(v)|)\sqrt{d}}. \quad (18)$$

The stability conditions of the other order RK _{m'} -MRTD-D _{m'} algorithm are derived as the same procedure of the RK₄-MRTD-D₄, which was not described here for simplicity.

The maximum Courant-Friedrichs-Lewy (CFL) number of the HO-FDTD (2, 2M), MRTD, and RK-MRTD methods are listed in Table 3, and the Dubechies D _{m'} ($m' = 2, 3, 4$) and Coifman basis are used in the MRTD and RK-MRTD methods. It is found that the higher order in the spatial and temporal discretizations, the more strict stability condition required, but the RK₄-MRTD-D₄ is less restrictive than any other method, and the RK₂-MRTD-D₂ is unconditionally unstable.

Table 3: The maximum CFL number for the HO-FDTD, MRTD, and RK-MRTD method.

	HO-FDTD	MRTD	RK-MRTD
(2,6) / D2	0.4650	0.4330	-
(2,10) / D3	0.4385	0.3951	0.3422
(2,14) / D4	0.4256	0.3802	0.5377
(2,16) / coif	0.4213	0.3802	0.53770

B. Dispersion

The dispersion characteristics are typically derived by assuming a time harmonic plane wave solution in an isotropic, linear, and lossless medium. The dispersion relation for the arbitrary HO-FDTD (2N, 2M) [7] method can be written as,

$$\left[\sum_{v=1}^N a(v) \sin\left(\frac{(2v-1)\omega \Delta t}{2}\right) \right]^2 =$$

$$= \left[\frac{c \Delta t}{\Delta x} \sum_{v=1}^M a(v) \sin\left(\frac{(2v-1)k_x \Delta x}{2}\right) \right]^2 \quad (19)$$

$$+ \left[\frac{c \Delta t}{\Delta y} \sum_{v=1}^M a(v) \sin\left(\frac{(2v-1)k_y \Delta y}{2}\right) \right]^2$$

$$+ \left[\frac{c \Delta t}{\Delta z} \sum_{v=1}^M a(v) \sin\left(\frac{(2v-1)k_z \Delta z}{2}\right) \right]^2$$

where k is the numerical wave number vector, λn is the numerical wavelength, its components are $k_x = k \sin \theta \cos \phi$, $k_y = k \sin \theta \sin \phi$, $k_z = k \cos \theta$. (θ, ϕ) is the wave propagation angle in the spherical coordinate, the uniform spatial step size is assumed as $\Delta x = \Delta y = \Delta z = \Delta$. Defining the CFL number $q = (c \Delta t) / \Delta$ and the number of cells per wavelength $p = \lambda c / \Delta$. The ratio of the theoretic wavelength value λc to the numerical wavelength λn is defined as $u = \lambda c / \lambda n$. Therefore, the dispersion relationship can be written as,

$$\left(\frac{1}{q} \sum_{v=1}^N a(v) \sin\left(\frac{\pi q}{p} \sin(2v-1)\right) \right)^2 =$$

$$= \left(\sum_{v=1}^M a(v) \sin\left(\frac{\pi u}{p} (2v-1) \sin \theta \cos \phi\right) \right)^2 \quad (20)$$

$$+ \left(\sum_{v=1}^M a(v) \sin\left(\frac{\pi u}{p} (2v-1) \sin \theta \sin \phi\right) \right)^2$$

$$+ \left(\sum_{v=1}^M a(v) \sin\left(\frac{\pi u}{p} (2v-1) \cos \theta\right) \right)^2.$$

With the same procedure above, the dispersion relation for the MRTD [11] method can be obtained as follows,

$$\left(\frac{1}{q} \sin\left(\frac{\pi q}{p}\right) \right)^2 = \left(\sum_{i=1}^{Nv-1} a(i) \sin\left(\frac{\pi u}{p} (2i-1) \sin \theta \cos \phi\right) \right)^2$$

$$+ \left(\sum_{i=1}^{Nv-1} a(i) \sin\left(\frac{\pi u}{p} (2i-1) \sin \theta \sin \phi\right) \right)^2$$

$$+ \left(\sum_{i=1}^{Nv-1} a(i) \sin\left(\frac{\pi u}{p} (2i-1) \cos \theta\right) \right)^2. \quad (21)$$

The dispersion of the RK-MRTD needs to use the theory of the SSP-RK [24], take RK₃-MRTD-D₃ for example, and according to [25], by substituting equations (11) and (16) in to equation

(22), then the dispersion relation can be derived in equation (23) as,

$$\omega t = \text{Arg}(\sigma) \tag{22}$$

$$\left(\frac{2\pi q}{up}\right)^2 = \left(\arctan\left(\frac{6\lambda_i\Delta t - (\lambda_i\Delta t)^3}{6 - 3(\lambda_i\Delta t)^2}\right)\right)^2. \tag{23}$$

With the wave propagation angle $\theta=90^\circ$ and $\phi=0^\circ$, CFL number $q = 0.25$. Figures (1) to (3) show the dispersion error Vn/c versus the number of cells per wavelength p for different methods in 3D. A summarized performance of the three methods is presented in Fig. 4.

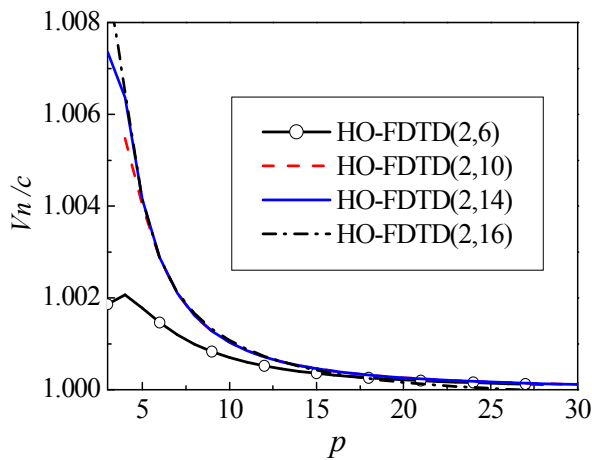


Fig. 1. Dispersion error of the HO-FDTD method.

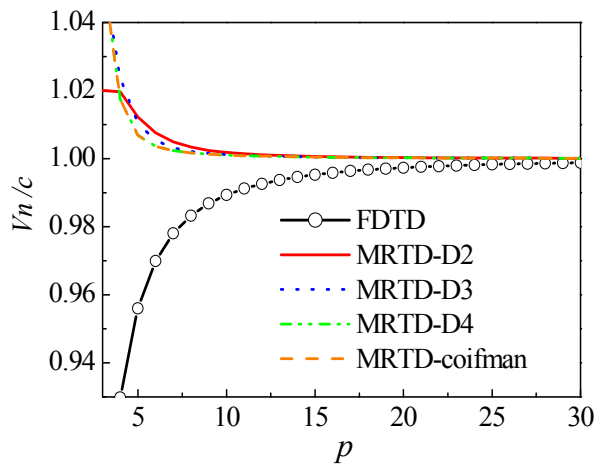


Fig. 2. Dispersion error of the MRTD methods.

Figure 1 shows the dispersion error Vn/c , where Vn refers to the numerical phase velocity, for the HO-FDTD (2, 6), (2, 10), (2, 14), (2, 16).

With increasing p , the HO-FDTD (2, 16) is obviously superior to the other three low order schemes (2, 6), (2, 10), and (2, 14), especially when p is larger than 17.

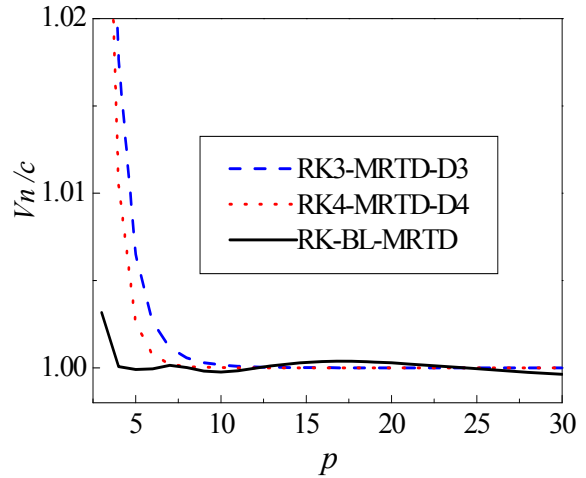


Fig. 3. Dispersion error of the RK-MRTD method.

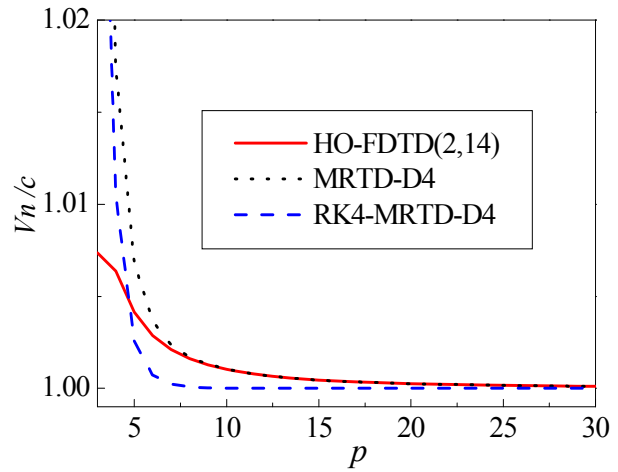


Fig. 4. Dispersion error of the different methods.

Figures 5 to 9 show the dispersion error versus the wave propagation angle ϕ for $\theta = 90^\circ$ and $\Delta x = \Delta y = \Delta z = \Delta = \lambda / 5$. From the figures, we can see that: (i) the larger the stencil spatial size the minimum is the dispersion error for the same method; (ii) for different methods and with the same spatial stencil size, the HO-FDTD and RK-MRTD method both provide the better dispersion characteristics than their corresponding MRTD counterparts.

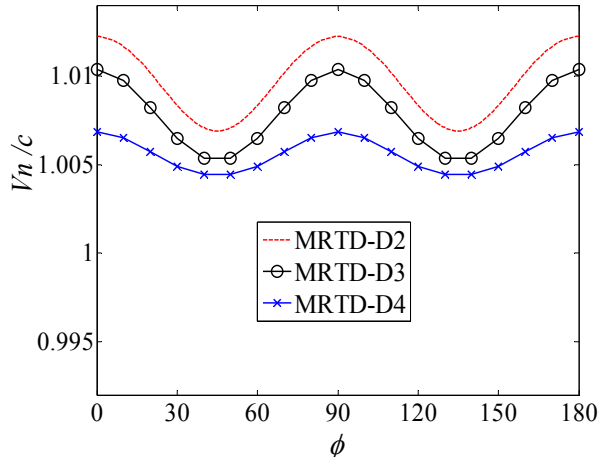


Fig. 5. Dispersion error versus ϕ for the MRTD methods.

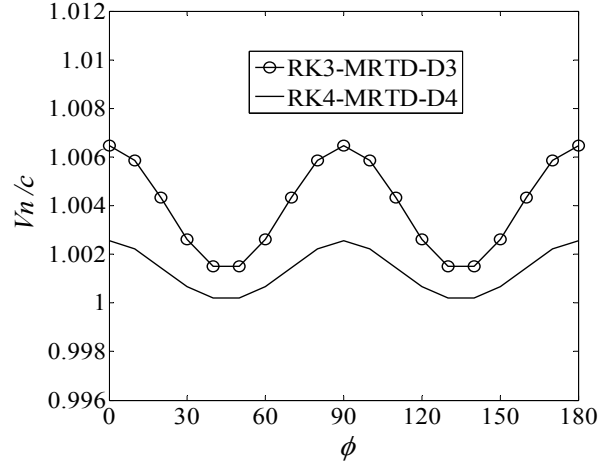


Fig. 8. Dispersion error versus ϕ of the RK-MRTD methods.

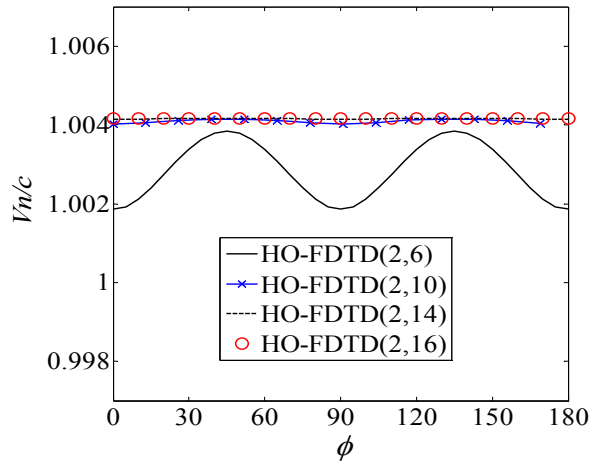


Fig. 6. Dispersion error versus ϕ of the HO-FDTD method.

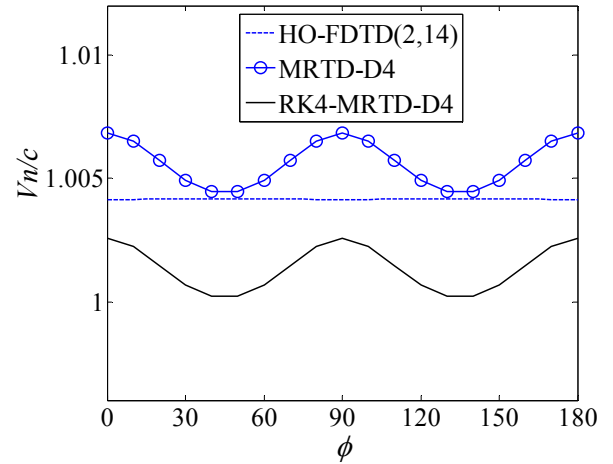


Fig. 9. Dispersion error versus ϕ of the different methods.

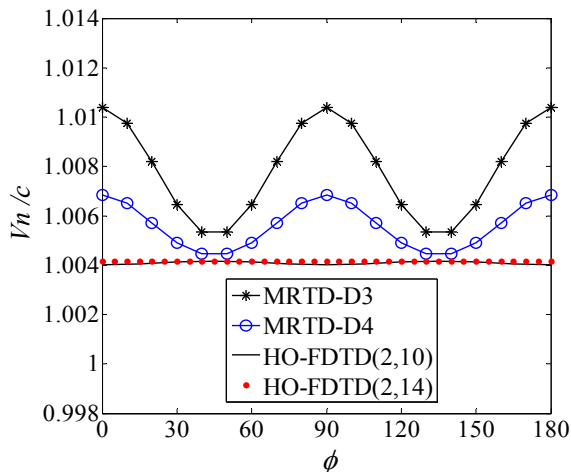


Fig. 7. Dispersion error versus ϕ of the MRTD and HO-FDTD methods.

C. Convergence

Because the HO-FDTD method uses Taylor series to expand the Maxwell's equations, the arbitrary HO-FDTD $(2N, 2M)$ schemes employ the $2N^{\text{th}}$ -order Taylor series expansion in time and the $2M^{\text{th}}$ -order Taylor series expansion in space, therefore,

$$\left\| f - \sum \frac{f^N(t)}{N!} (\Delta t)^N \right\| \leq C_n (\Delta t)^n \|f^n\| \quad (24)$$

$$\left\| f - \sum \frac{f^M(x)}{M!} (\Delta x)^M \right\| \leq C_m (\Delta x)^m \|f^m\|, \quad (25)$$

$$R_{r'}(\zeta) = \frac{f^{r'}(\zeta)}{r'!} (\Delta \zeta)^{r'} = C_{r'} (\Delta \zeta)^{r'} \|f^{r'}\|, \\ \lim_{r' \rightarrow \infty} R_{r'}(\zeta) = 0, \quad (26)$$

where equation (26) is the Taylor series remainder, $C_{\bar{n}}$, $C_{\bar{m}}$ and $C_{\bar{r}}$ are the coefficients, so the error is a convergence relation that can be written as the RK-MRTD in [6],

$$\text{HO-FDTD } (2N, 2M)\text{-error} \leq A' \Delta t^{\bar{n}} + B' \Delta x^{\bar{m}}. \quad (27)$$

Thus, the convergence relation of HO-FDTD (2, 2M) scheme can be derived as,

$$\text{HO-FDTD } (2, 2M)\text{-error} \leq C' \Delta t^2 + B' \Delta x^{m'} \quad (28)$$

where A' , B' , and C' are the constant coefficients. Take the Daubechies N' scaling functions, for example, and the CFL stability condition $\Delta t = q\Delta x/c$ ($q \leq 1$), then the convergence relation of the MRTD schemes [6] can be derived as,

$$\begin{aligned} \text{MRTD-error} &\leq A\Delta x^{N'} + B\Delta t^2 \\ &\leq A\Delta x^{N'} + B\left(\alpha \frac{\Delta x}{c}\right)^2 \leq C\Delta x^2. \end{aligned} \quad (29)$$

The RK-MRTD method based on the MRTD uses the m^{th} -order m' stage SSP-RK method in temporal discretization. It is known in [6] that

$$\text{RK-MRTD error} \leq C_t \Delta t^{m'} + C_x \Delta x^{N'}, \quad (30)$$

simplified and summarized as,

$$\text{RK-MRTD -error} \leq C_N \Delta x^{N'}. \quad (31)$$

From Fig. 10, it is easily to find the RK-MRTD scheme based on Daubechies basis functions that have the higher temporal and spatial convergence than other cases.

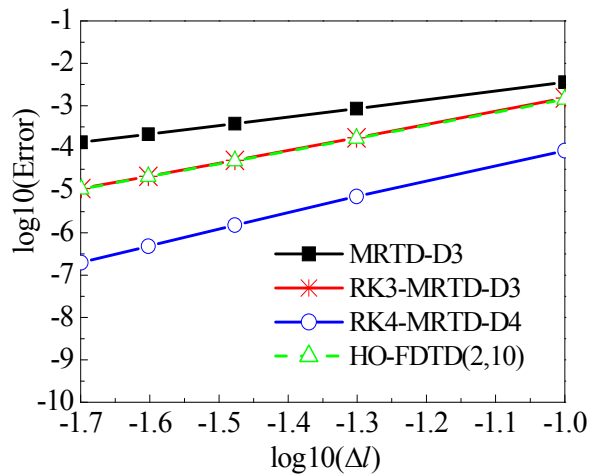


Fig. 10. Convergence of the MRTD, HO-FDTD, and RK-MRTD methods.

IV. COMPUTATIONAL COST AND MEMORY REQUIREMENTS

Here, we analyze and discuss the computational cost and memory requirements of the HO-FDTD (2, 2M), MRTD and RK-MRTD method. As in [6], for 3D case, the fields at a final time for the HO-FDTD (2, 2M) and MRTD methods only E^n and $H^{n-1/2}$ need to be stored at each time step, while the RK-MRTD method demand to store the values of $F^{(i)}$ and F_{n+1} , so the memory requirements of the RK-MRTD method are twice that of the other two methods.

The computational cost of the MRTD method [6] for a single time step is,

$$\text{Cost}_{\text{MRTD}} = 2(n_1)^3 \times (4N' - 2) \quad (32)$$

where N' is the order of the scaling function $D_{N'}$, n_1 is the number of cells in a single direction. If the domain is the unit size, then $n_1 = 1/\Delta x_1$, and Δx_1 is the grid spacing. Similarly, the computational cost of the HO-FDTD (2, 2M) method is,

$$\text{Cost}_{\text{HO-FDTD}} = 2(n_2)^3 \times 2M \quad (33)$$

where n_2 is the number of the cells in a single direction, $n_2 = 1/\Delta x_2$ for unit size and Δx_2 is the grid spacing for the HO-FDTD (2, 2M) method. We know that the RK-MRTD method base on the m' stage m^{th} -order SSP-RK algorithm (cf. (5)), for a single time step, the computational cost [6] is,

$$\text{Cost}_{\text{RK-MRTD}} = 2(n_{m'})^3 \times m' \times (4N' - 1) \quad (34)$$

where $n_{m'}$ is the number of the cells in a single direction, $n_{m'} = 1/\Delta x_{m'}$ for unit size and $\Delta x_{m'}$ is the grid spacing for the RK-MRTD method.

From equations (32) and (33), we found that the MRTD and HO-FDTD (2, 2M) methods have the same computational cost if they have the same number of the cells in a single direction and the spatial stencil size. If the computational domain is unit size, and Δt_1 is the maximal stable time step for the MRTD method and $m' = N'$, the time step $\Delta t_{N'}$ for the RK-MRTD must be chosen as $\Delta t_{N'} = 2\Delta t_1 / N'$, the same as the HO-FDTD method, Δt_2 is the maximal stable time step for the HO-FDTD (2, 2M) method and the time step must be chosen as $\Delta t_{N'} = 2\Delta t_2 / N'$. If the total computational time is 1, then the cost of the three methods are,

$$\text{Cost}_{\text{MRTD}} = 2(n_1)^3 \times (4N' - 2) \times \frac{1}{\Delta t_1} \quad (35)$$

$$\mathbf{Cost}_{\text{HO-FDTD}} = 2(n_2)^3 \times 2M \times \frac{1}{\Delta t_2} \quad (36)$$

$$\begin{aligned} \mathbf{Cost}_{\text{RK-MRTD}} &= 2(n_{m'})^3 \times m' \times (4N'-1) \times \frac{1}{\Delta t_{N'}} \\ &= 2(n_{m'})^3 \times N' \times (4N'-1) \times \frac{1}{\Delta t_{N'}} \\ &= (n_{m'})^3 \times (N')^2 \times (4N'-1) \times \frac{1}{\Delta t_1} \\ &= (n_{m'})^3 \times (N')^2 \times (4N'-1) \times \frac{1}{\Delta t_2}. \end{aligned} \quad (37)$$

For a given accuracy, and using the above equations, the computational cost relations among the MRTD, HO-FDTD, and RK-MRTD methods can be derived as,

$$\begin{aligned} \mathbf{Cost}_{\text{RK-MRTD}} &= 2(n_{m'})^3 \times N' \times (4N'-1) \times \frac{1}{\Delta t_{N'}} \\ &= (n_{m'})^3 \times (N')^2 \times (4N'-1) \times \frac{1}{\Delta t_1} \\ &= \left(\frac{n_{m'}}{n_1} \right)^3 \frac{(N')^2 \times (4N'-1)}{2(4N'-2)} \times \left(2(n_1)^3 \times (4N'-2) \times \frac{1}{\Delta t_1} \right) \\ &= \eta_1 \times (\mathbf{Cost}_{\text{MRTD}}) \end{aligned} \quad (38)$$

$$\begin{aligned} \mathbf{Cost}_{\text{RK-MRTD}} &= 2(n_{m'})^3 \times N' \times (4N'-1) \times \frac{1}{\Delta t_{N'}} \\ &= (n_{m'})^3 \times (N')^2 \times (4N'-1) \times \frac{1}{\Delta t_2} \\ &= \left(\frac{n_{m'}}{n_2} \right)^3 \frac{(N')^2 \times (4N'-1)}{4M} \times \left(2(n_2)^3 \times 2M \times \frac{1}{\Delta t_2} \right) \\ &= \eta_2 \times (\mathbf{Cost}_{\text{HO-FDTD}}), \end{aligned} \quad (39)$$

where

$$\eta_1 = \left(\frac{n_{m'}}{n_1} \right)^3 \frac{(N')^2 \times (4N'-1)}{2(4N'-2)} \quad (40)$$

$$\eta_2 = \left(\frac{n_{m'}}{n_2} \right)^3 \frac{(N')^2 \times (4N'-1)}{4M}, \quad (41)$$

where η_1 and η_2 are constants dependent on $n_{m'}$, n_1 , N' , n_2 , and M . From equations (38) and (39), we know that the computational time of the RK-MRTD method is η_1 times of the MRTD and η_2 times of the HO-FDTD method, and η_1 , η_2 can be controllable.

V. NUMERICAL EXAMPLE

In this section, the three above methods will be validated via a simple classical metal sphere scattering example. The radius of the sphere is 1 m, and illuminated by a Gaussian pulse at a Gaussian pulse at $\theta = 0^\circ$, $\varphi = 90^\circ$, and the polarization of the electric field along x -direction with increasing centre frequencies from 1 MHz to 300 MHz. The CFL number is 0.3, the cell size $\Delta = 0.05$ m, the time step size $\Delta t = 0.3 \Delta / c$, and the total computational time is 2000 steps. Backward scattering RCS for different methods of the metal sphere are shown in Fig. 11, including the Mie series solution, HO-FDTD (2, 14), MRTD-D₄ and RK₄-MRTD-D₄. From the Fig. 11, we can see that errors are increased with increasing the centre frequency because the number of per wavelength decreases with increasing the centre frequency for fixed cell size. But in the lower frequency part, the RK₄-MRTD-D₄ method is better in comparison with the Mie series solution than other methods. The results also agree with those shown in Figs. 4 and 9.

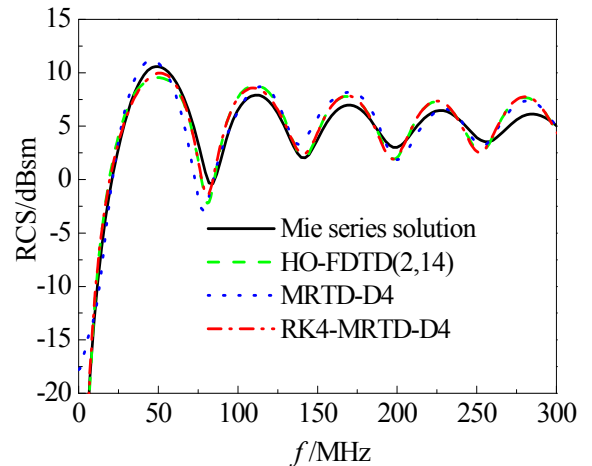


Fig. 11. Backward scattering RCS of the metal sphere.

Figure 12 shows the convergence of the metal sphere scattering in a 3D case. From the figure, we can see that the convergence rate of the RK₄-MRTD-D₄, MRTD-D₄, and HO-FDTD (2, 14) are 4, 2, 2, respectively, and the RK₄-MRTD-D₄ is faster than the other two methods, which are in accordance with the conclusion in Fig. 10.

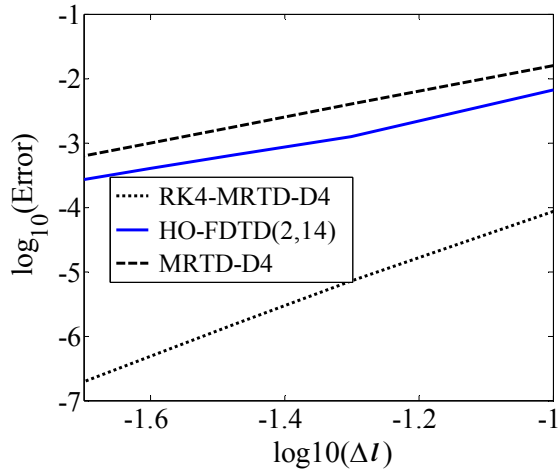


Fig. 12. Convergence of different methods for the scattering of a metal sphere in a 3D case.

VI. CONCLUSION

In this paper, the stability, numerical dispersion, and convergence of the HO-FDTD, MRTD, and RK-MRTD schemes have been investigated, respectively. Analytical stability condition expression for the arbitrary HO-FDTD ($2N, 2M$) method has been derived. It is proved that the HO-FDTD schemes have less restrictive conditions of the stability than those of the MRTD method. The dispersion relation for the RK-MRTD schemes also has been derived. It is found, that for the same scheme, for example the HO-FDTD schemes, finer discretizations in time and space domains can decrease the numerical dispersion; among different methods the RK-MRTD schemes demonstrate better dispersion than the HO-FDTD and MRTD methods. The computational cost and memory requirements are discussed in this paper. In section V, a simple and classical example has been used to prove that these methods have certain research value, especially the RK-MRTD method, which has both the better numerical properties and controllable computational time. The conclusions demonstrate that the RK-MRTD method has the potential ability and research significance in computational electromagnetics.

ACKNOWLEDGMENT

This work was supported by the National Nature Science Foundation of China under Contract 61172024. It was also supported by the

Funding of Jiangsu Innovation Program for Graduate Education and the Fundamental Research Funds for the Central Universities under Contract cxzz12-0156.

REFERENCES

- [1] K. S. Yee, "Numerical solution of initial boundary value problems involving Maxwell's equation in isotropic media," *IEEE Trans. Antennas Propagat.*, vol. 14, no.3, pp. 302-307, May1966.
- [2] J. Fang, *Time Domain Finite Difference Computation for Maxwell's Equation*, Ph.D. Dissertation, University of California at Berkeley, Berkeley, CA, 1989.
- [3] C. W. Manry, S. L. Broschat, and J. B. Schneider, "High-order FDTD methods for large problems," *Appl. Comp. Electro. Soc. Journal*, vol. 10, no. 2, pp. 17-29, 1995.
- [4] D. W. Zingg, "Comparison of the high-accuracy finite difference methods for linear wave propagation," *SIAM Journal Sci. Comput.*, vol. 22, no. 2, pp. 476-502, 2000.
- [5] M. Krumpholz and L. P. B. Katehi, "MRTD: New time-domain schemes based on multiresolution analysis," *IEEE Trans. Microw. Theory Tech.*, vol. 44, pp. 555-571, Apr. 1996.
- [6] Q. Cao, R. Kanapady, and F. Reitich, "High-order Runge-Kutta multiresolution time-domain methods for computational electromagnetics," *IEEE Trans. Microw. Theory Tech.*, vol. 54, no. 8, pp. 3316-3326, Aug. 2006.
- [7] J. Zhang and Z. Chen, "Low-dispersive super high-order FDTD schemes," *IEEE Antennas and Propagation Society International Symposium*, vol. 3, pp. 1510-1513, 2000.
- [8] L. Kuzu, M. Gokten, A. Yagli, V. Yanikgonul, and E. Demircioglu, "Fourth-order accurate FDFD method for general waveguide structures," *28th Annual Review of Progress in Applied Computational Electromagnetics Society*, pp. 405-410, Columbus, Ohio, April 2012.
- [9] M. Aidam and P. Russer, "Application of biorthogonal B-spline wavelets to Telegrapher's equations," *Proc. of the 14th Annual Review of Progress in Applied Computational Electromagnetics Society*, pp. 983-990, Monterey, CA, March 1998.
- [10] E. M. Tentzeris, R. L. Robertson, and J. F. Harvey, et al, "Stability and dispersion analysis of battle-lemarie-based MRTD schemes," *IEEE Trans. Microw. Theory Tech.*, vol. 47, no. 7, pp. 1004-1013, July. 1999.
- [11] M. Fujii and W. J. R. Hofer, "Dispersion of time-domain wavelet Galerkin method based on Daubechies compactly supported scaling

- functions with three and four vanishing moments,” *IEEE Microwave Guided Wave Lett.*, vol. 10, no. 7, pp. 1752-1760, July 2002.
- [12] T. Dogaru and L. Carin, “Multiresolution time-domain using CDF biorthogonal wavelets,” *IEEE Trans. Microw. Theory Tech.*, vol. 49, no. 5, pp. 902-3912, May 2001.
- [13] X. Zhu, T. Dogaru, and L. Carin, “Three-dimensional biorthogonal multiresolution time-domain method and its application to scattering problems,” *IEEE Trans. Microw. Theory Tech.*, vol. 51, no. 5, pp. 1085-1092, May 2003.
- [14] H. I. Resnikoff and R. O. Wells Jr., *Wavelet Analysis*, Spring, New York, NY, 1998.
- [15] A. Alighanbari and C. D. Sarris, “Dispersion properties and applications of the Coifman scaling function based S-MRTD,” *IEEE Trans. Antennas Propagat.*, vol. 54, no. 8, pp. 2316-2325, Aug. 2006.
- [16] Q. Cao and K. Tamma, “Multiresolution time domain for studies of planar stratified media,” *19th Annual Review of Progress in Applied Computational Electromagnetics Society*, pp. 669-672, Monterey, CA, March 2003.
- [17] Q. Cao and K. K. Tamma, “Multiresolution time domain based different wavelet basis studies of scattering of planar stratified medium and rectangular dielectric cylinder,” *Appl. Comp. Electro. Society Journal*, vol. 20, no. 1, pp. 86-95, March 2005.
- [18] M. Tentzeris and N. Bushyager, “Practical considerations in the MRTD modeling of microwave structures,” *21st Annual Review of Progress in Applied Computational Electromagnetics Society*, Honolulu, Hi, 2005.
- [19] C. Represa, C. Pereira, A. C. L. Cabeceira, I. Barba, and J. Represa, “PML absorbing boundary conditions for the multiresolution time-domain techniques based on the discrete wavelet transform,” *Appl. Comp. Electro. Society (ACES) Journal*, vol. 20, no. 3, pp. 207-212, Nov. 2005.
- [20] S. Gottlieb, C. -W. Shu, and E. Tadmor, “Strong stability-preserving high-order time discretization methods,” *SIAM Rev.*, vol. 43, no. 1, pp. 89-112, 2001.
- [21] M. -H. Chen, B. Cockburn, and F. Reitich, “High-order RKDG methods for computational electromagnetics,” *Journal of Sci. Comput.*, vol. 22/23, no. 1-3, pp. 205-226, June 2005.
- [22] Y. Liu, “Fourier analysis of numerical algorithms for the Maxwell’s equation,” *Journal of Comput. Phys.*, vol. 124, pp. 396-416, 1996.
- [23] X. Chen and Q. Cao, “Analysis of characteristics of two-dimensional Runge-Kutta multiresolution time-domain scheme,” *Progress In Electromagnetics Research M*, vol. 13, pp. 217-227, 2010.
- [24] S. Zhao and G. W. Wei, “High-order FDTD methods via derivative matching for Maxwell’s equations with material interfaces,” *Journal Comput. Phys.*, vol. 200, pp. 60-103, Oct. 2004.
- [25] G. Sun and C. W. Trueman, “Analysis and numerical experiments on the numerical dispersion of two-dimensional ADI-FDTD,” *IEEE Antennas and Wireless Propagat. Lett.*, vol. 2, pp.78-81, 2003.